Published in final edited form as:
Am J Ophthalmol. 2009 July ; 148(1): 155–63.e1. doi:10.1016/j.ajo.2009.01.021.

Impact of Atypical Retardation Patterns on Detection of Glaucoma Progression using the GDx with Variable Corneal Compensation

FELIPE A. MEDEIROS, **LUCIANA M. ALENCAR**, **LINDA M. ZANGWILL**, **PAMELA A. SAMPLE**, **REMO SUSANNA JR**, and **ROBERT N. WEINREB**
Hamilton Glaucoma Center and Department of Ophthalmology, University of California, San Diego, La Jolla, California (F.A.M., L.M.A., L.M.Z., P.A.S., R.N.W.); and the Department of Ophthalmology, University of São Paulo, São Paulo, Brazil (L.M.A., R.S.).

Abstract

PURPOSE—To evaluate the impact of atypical retardation patterns (ARP) on detection of progressive retinal nerve fiber layer (RNFL) loss using scanning laser polarimetry with variable corneal compensation (VCC).

DESIGN—Observational cohort study.

METHODS—The study included 377 eyes of 221 patients with a median follow-up of 4.0 years. Images were obtained annually with the GDx VCC (Carl Zeiss Meditec Inc, Dublin, California, USA), along with optic disc stereophotographs and standard automated perimetry (SAP) visual fields. Progression was determined by the Guided Progression Analysis software for SAP and by masked assessment of stereophotographs by expert graders. The typical scan score (TSS) was used to quantify the presence of ARPs on GDx VCC images. Random coefficients models were used to evaluate the relationship between ARP and RNFL thickness measurements over time.

RESULTS—Thirty-eight eyes (10%) showed progression over time on visual fields, stereophotographs, or both. Changes in TSS scores from baseline were significantly associated with changes in RNFL thickness measurements in both progressing and nonprogressing eyes. Each 1-unit increase in TSS score was associated with a 0.19-μm decrease in RNFL thickness measurement ($P < .001$) over time.

CONCLUSIONS—ARPs had a significant effect on detection of progressive RNFL loss with the GDx VCC. Eyes with large amounts of atypical patterns, great fluctuations on these patterns over time, or both may show changes in measurements that can appear falsely as glaucomatous progression or can mask true changes in the RNFL.

SCANNING LASER POLARIMETRY IS DESIGNED TO PROvide real-time objective measurements for assessing the thickness of the retinal nerve fiber layer (RNFL). It is based on the principle that the birefringent RNFL induces a change in retardation of passing polarized light that is proportional to its thickness.[1] Because the cornea (nd to a lesser extent the lens) also exhibits birefringence and induces retardation on polarized light, it needs to be neutralized to extract the RNFL retardation from the total retardation in a particular eye. Initial versions of the scanning laser polarimetry technology used a fixed method of corneal compensation, which assumed all individuals to have similar magnitudes and axis of corneal polarization. Because the scanning laser polarimetry with fixed corneal compensation was shown to obtain spurious RNFL measurements in many eyes, a variable corneal compensator (VCC) was

Inquiries to Felipe A. Medeiros, Hamilton Glaucoma Center, University of California, San Diego, 9500 Gilman Drive, La Jolla, CA 92093; fmedeiros@eyecenter.ucsd.edu.

developed and incorporated into the GDx VCC instrument (Carl Zeiss Meditec Inc, Dublin, California, USA), resulting in improved diagnostic accuracy.[2–8]

Soon after the introduction of the GDx VCC, however, scans showing atypical retardation patterns (ARP) were observed in some eyes imaged with this instrument. These scans show irregular patches of elevated retardation values that do not match the expected retardation based on the RNFL anatomic features. ARPs seem to result from poor signal-to-noise ratio as a consequence of light scattering in the eye.[9] To compensate for a decrease in signal, the instrument automatically increases the gain to augment the polarization signal, which paradoxically increases the noise from deeper structures such as the sclera. Using subjective evaluation, Bagga and associates found ARPs in 25% of normal and in 51% of glaucomatous eyes.[10] Moreover, their presence seems to have an adverse effect on the diagnostic performance of the GDx VCC. Bowd and associates showed that the performance of the GDx VCC for glaucoma diagnosis decreases significantly when ARPs are present.[11]

Although ARPs have been demonstrated to result in low diagnostic accuracy to discriminate glaucomatous from normal eyes, their effect on longitudinal measurements obtained with the GDx VCC has not yet been studied. If the atypical patterns do not change significantly over time, it is possible that they would not exert a significant influence on the detection of progressive RNFL loss with this instrument. In a previous study, we demonstrated that the GDx VCC is able to detect progressive RNFL loss in a cohort of glaucoma eyes and eyes suspected of having the disease with scans showing minimal or no ARPs.[12] In the current study, we expanded our cohort to include eyes with a large range of ARP severities, and we investigated changes in ARPs over time and their influence on the detection of progressive RNFL loss with this instrument.

METHODS

THIS WAS AN OBSERVATIONAL COHORT STUDY. PARTICIpants from this study were included in a prospective, longitudinal study designed to evaluate optic nerve structure and visual function in glaucoma, the Diagnostic Innovations in Glaucoma Study conducted at the Hamilton Glaucoma Center, University of California, San Diego. Participants in the Diagnostic Innovations in Glaucoma Study were evaluated longitudinally according to a preestablished protocol that included regular follow-up visits in which patients underwent clinical examination and several other imaging and functional tests. All the data were entered in a computer database. All participants from the Diagnostic Innovations in Glaucoma Study who met the inclusion criteria described below were enrolled in the current study. Informed consent was obtained from all participants.

At each visit during follow-up, subjects underwent a comprehensive ophthalmologic examination including review of medical history, best-corrected visual acuity (BCVA), slit-lamp biomicroscopy, intraocular pressure (IOP) measurement, gonioscopy, dilated funduscopic examination, stereoscopic optic disc photography, and automated perimetry using either 24-2 full-threshold or Swedish interactive threshold algorithm. Only subjects with open angles on gonioscopy were included. Subjects were excluded if they presented BCVA less than 20/40; spherical refraction outside ± 5.0 diopters (D), cylinder correction outside 3.0 D, or both; or any other ocular or systemic disease that could affect the optic nerve or the visual field (VF).

The study included patients diagnosed with glaucoma as well as patients suspected of having the disease, as determined on the baseline visit. Eyes were classified as glaucomatous if they had repeatable (2 consecutive) abnormal VF test results on the baseline visits, defined as a pattern standard deviation (SD) outside of the 95% normal confidence limits, or glaucoma

hemifield test results outside normal limits, regardless of the appearance of the optic disc. VFs were reviewed by a glaucoma specialist (F.A.M.) masked to the results of the other tests to determine whether VF defects had a glaucomatous pattern and were repeatable (ie, occurred on the same location). Eyes were classified as glaucoma suspects if they had a history of elevated IOP (> 21 mm Hg), suspicious or glaucomatous appearance of the optic nerve but normal and reliable VF results on the baseline visits, or both. If both eyes from the same patient were eligible for the study, both eyes were included in the analysis, and statistical procedures were used to take into account the correlation between measurements within the same patient.

A minimum follow-up period of 1 year with the GDx VCC and a minimum of 3 separate visits were required in the study. GDx VCC images were obtained annually during follow-up. Eligible subjects were required to have had a VF examination and optic disc stereophotographs obtained close in time to the baseline and last GDx VCC scans. Baseline was set at the first occurrence of this matching, and the GDx VCC date was used as the baseline date. During follow-up, each patient was treated at the discretion of the attending ophthalmologist.

The median follow-up time was 4.0 years (first quartile, 3.1 years; third quartile, 4.5 years). The study included a total of 1,814 GDx VCC visits. The number of visits per eye ranged from 3 to 8, with 92% of the eyes having at least 4 visits and 64% having at least 5 visits during follow-up.

SCANNING LASER POLARIMETRY

Patients were imaged using a commercially available scanning laser polarimeter with variable corneal compensation (GDx VCC, software version 5.5.1; Carl Zeiss Meditec Inc). The general principles of scanning laser polarimetry and the algorithm used for variable corneal compensation have been described in detail elsewhere.[1,2,13] Because corneal polarization axis and magnitude affect scanning laser polarimetry measurements and are not similar in all eyes, the GDx VCC uses a variable corneal polarization compensator that allows eye-specific compensation of anterior chamber birefringence. After determining the axis and magnitude of corneal polarization in each eye by macular scanning,[2] an appropriately compensated retinal polarization image is automatically obtained and available for analysis. Assessment of GDx VCC image quality was performed by an experienced examiner masked to the subject's identity and results of the other tests. To be classified as good quality, an image required a focused and evenly illuminated reflectance image with a centered optic disc and a quality score no lower than 7.

GDx VCC parameters provided in the standard printout of the instrument and investigated in this study were superior average, inferior average, temporal–superior–nasal–inferior–temporal (TSNIT; circumpapillary RNFL thickness measured under the automatically defined 3.2-mm diameter calculation circle) average, TSNIT SD, and the nerve fiber indicator (NFI). The NFI is calculated using a support vector machine algorithm based on several RNFL measures and assigns a number from 0 to 100 to each eye. According to the manufacturer, the higher the NFI, the greater the likelihood the patient has glaucoma.

To quantify the presence of ARPs on GDx VCC scans, we used the software-provided parameter typical scan score (TSS). The TSS is a continuous variable ranging from 0 to 100 and is the result of a support vector machine analysis of scanning laser polarimetry data labeled for training based on the subjective appearance of each scan (typical vs atypical). TSS is based on the slope, SD and average magnitude of RNFL thickness measurements from the edge of the optic disc extending outward to 20 degrees. Low TSS scores indicate atypical scans and high TSS scores indicate typical ones.

ASSESSMENT OF CHANGE USING OPTIC DISC STEREO-PHOTOGRAPHS AND STANDARD AUTOMATED PERIMETRY

Simultaneous stereoscopic optic disc photographs (TRC-SS; Topcon Instrument Corp of America, Paramus, New Jersey, USA) were reviewed using a stereoscopic viewer (Asahi Pentax Stereo Viewer II; Asahi Optical Co, Tokyo, Japan). For progression assessment, each patient's most recent stereophotograph was compared with the baseline one. Each grader was masked to the temporal sequence of the photographs. Definition of change was based on focal or diffuse thinning of the neuroretinal rim, increased excavation, appearance, or enlargement of RNFL defects. Discrepancies between the 2 graders were resolved either by consensus or by adjudication of a third experienced grader (F.A.M.). Only photographs with adequate quality were included. Fifteen eyes of 221 patients were excluded because of poor quality photographs that did not allow evaluation of progression.

Standard automated perimetry (SAP) VFs were obtained using the Swedish interactive threshold algorithm (Humphrey Field Analyzer; Carl Zeiss Meditec Inc) strategy. Only reliable test results (≤ 33% fixation losses and false-negative results and < 15% false-positive results) were included. Glaucomatous VF progression was assessed using the Humphrey Field Analyzer Guided Progression Analysis software. Progression by SAP Guided Progression Analysis was defined as a significant decrease from baseline (2 examinations) pattern deviation at 3 or more of the same test points on 3 consecutive tests.[14]

STATISTICAL ANALYSIS

Random coefficients models were used to evaluate the relationship between atypical patterns of retardation and RNFL thickness measurements over time. These models are a type of linear mixed model that involves both random intercepts and random slopes and that takes into account the clustered structure of the data, allowing the residuals associated with the longitudinal measures on the same unit of analysis to be correlated.[15,16]

The model was built as follows. GDx VCC RNFL thickness measurements were considered as the dependent variable. A variable termed ΔTSS was calculated as the difference between the TSS value for a particular examination during follow-up and the TSS at the baseline examination for the same eye. This variable was entered as a fixed-effects covariate and represented the change in TSS from the baseline visit. Therefore, its coefficient indicated the impact that changes in atypical patterns of retardation had on GDx VCC RNFL measurements over time. A variable termed *TSS and the interaction term with time* (TSS × TIME) were included as fixed-effects covariates to evaluate whether there was an influence of the baseline TSS value (ie, the amount of atypia in the baseline scan) on detection of RNFL loss over time with the GDx VCC.

Progression as assessed by stereophotographs and SAP was included as a fixed-effect covariate (variable PROG in the model below) with a value of 1 if the eye progressed by stereophotographs, SAP, or both and a value of 0 if the eye did not show progression with any of these methods. Time (variable TIME) was included as a continuous predictor. The significance of the coefficient associated with the variable TIME indicates whether there was a significant trend in GDx measurements over time, that is, whether GDx measurements tended to decrease or increase significantly over time. The two-way interaction between TIME and PROG was included in the model to evaluate whether there was a significant difference in longitudinal GDx measurements over time between progressors and nonprogressors. Because our previous research indicated a significant effect of baseline measurements on the ability of the GDx VCC to detect change over time, a variable representing baseline GDx measurements (variable BASELINE) and the interaction term with time (BASELINE × TIME) also were included as fixed-effects covariates in the models.

The following random components were added to the model: random patient-specific effects associated with both the intercept and slope (ie, the effect of time) for each patient and random specific effects associated with both the intercept and slope for each eye nested within patient. The general form of the model for an individual GDx measurement at time *t* (*t* represents visit during follow-up) on eye *i* nested within patient *j* (denoted by GDx_{tij}) was as follows:

$$\begin{aligned} GDx_{tij} = {} & \beta_0+\beta_1 \times TSS_{ij}+\beta_2 \times TSS_{ij} \times TIME_{tij} \\ & +\beta_3 \times \Delta TSS_{tij}+\beta_4 \times TIME_{tij}+\beta_5 \times PROG_{ij} \\ & +\beta_6 \times PROG_{ij} \times TIME_{tij}+\beta_7 \times BASELINE_{ij} \\ & +\beta_8 \times BASELINE_{ij} \times TIME_{tij}+\zeta_{0j}+\zeta_{1j} \times TIME_{tij} \\ & +\zeta_{0i|j}+\zeta_{1i|j} \times TIME_{tij}+\varepsilon_{tij}. \end{aligned}$$

The parameters β_0 through β_8 represent the fixed effects associated with the intercept, TSS value at baseline, change in TSS from baseline, time, progression, baseline measurements, and their two-way interactions with time; ζ_{0j} and ζ_{1j} are random patient effects associated with the intercept and time slope, respectively; $\zeta_{0i|j}$ and $\zeta_{1i|j}$ are the random effects (intercept and slope, respectively) associated with eye nested within patient; and ε_{ytij} represents the residual.

Statistical analyses were performed using STATA software version 10.0 (StataCorp, College Station, Texas, USA) and SPSS software version 16.0 (SPSS Inc, Chicago, Illinois, USA). The α level (type I error) was set at 0.05.

RESULTS

THE STUDY INCLUDED 377 EYES OF 221 PATIENTS WITH A mean age ± SD of 65 ± 13 years. From the 377 eyes included in the study, 112 (30%) had a diagnosis of glaucoma and 265 (70%) were considered to be glaucoma suspects. Thirty-eight eyes (10%) showed progression over time on VFs, stereophotographs, or both. From the 38 progressing eyes, 16 (42%) progressed only by SAP Guided Progression Analysis, 15 (39%) progressed only by optic disc stereophotographs, and 7 (18%) progressed by both methods.

The average TSS score for all examinations of all eyes at baseline was 90 (median, 98; first quartile, 87; third quartile, 100). Sixty-five (18%) of 377 eyes had TSS scores at baseline lower than 80. Figure 1 shows a scatterplot of TSS and TSNIT average values at baseline. Lower TSS values were associated with higher TSNIT average measurements ($r = -0.26$; $P < .001$). A locally weighted scatterplot smoother (LOWESS) showed that the relationship between TSS and TSNIT average values was approximately linear. Each unit of TSS difference among eyes was associated with a 0.14-μm difference in TSNIT average at baseline.

Lower values of TSS at baseline were associated with greater change in TSS scores over time ($r = -0.27$; $P < .001$). When absolute changes in TSS scores from baseline were considered, eyes with lower TSS scores at baseline had greater absolute changes in TSS scores ($r = -0.56$; $P < .001$). That is, eyes with more atypical patterns at the baseline visits tended to have greater change in these patterns over time (Figure 2). For eyes with baseline TSS lower than 80, 52% of the 227 visits had a change of 10 units or more in TSS compared with the value in baseline. However, for eyes with baseline TSS of 80 or more, only 14% of the 1,210 visits had a change of 10 units or more in TSS compared with the value on the baseline visit.

Table 1 shows results of the random coefficient model for the parameter TSNIT average. There was a significant effect of TSS scores at baseline on GDx VCC RNFL thickness measurements over time. Eyes that had higher values of TSS at baseline (ie, scans with less ARPs) had more decrease in RNFL measurements over time. This is indicated by the statistically significant

coefficient attributed to the interaction term TSS × TIME (β_2; $P = .015$). Changes in TSS scores from baseline also were associated with changes in RNFL thickness measurements over time. Each 1-unit increase in TSS score (variable ΔTSS) was associated with a 0.19-μm decrease in RNFL thickness measurement (β_3; $P < .001$). The model also shows that patients who demonstrated progression by stereophotographs, VFs, or both had a significantly higher rate of RNFL loss over time, as indicated by the significant coefficient attributed to the interaction term PROG × TIME (β_6; $P = .002$). Controlling for TSS effects, the average rate of RNFL loss in progressing eyes was 0.65 μm/year compared with −0.19 μm/year for nonprogressing eyes. These values were estimated for average values of TSS and average values of baseline RNFL thickness measurements in the sample. We also tested whether there was a significant interaction between progression and TSS variables by including additional second-order interaction terms in the model (results not shown). None of these terms were significant, indicating that the effect of changes in TSS scores was similar in progressing and nonprogressing eyes.

Table 2 shows results of the models investigating the effect of TSS changes on other GDx VCC parameters. For the parameters superior average and inferior average, results were similar to those found for TSNIT average. A 1-unit change in TSS score over time induced a change of 0.13 μm for superior average ($P < .001$) and 0.11 μm for inferior average ($P < .001$). For the parameter NFI, a 1-unit increase in TSS over time resulted in 0.20 increase in NFI value ($P < .001$). Although the TSNIT SD parameter was less affected by changes in TSS over time ($P = .567$), this parameter was not able to discriminate progressing from nonprogressing eyes ($P = .135$ for the interaction term PROG × TIME).

Figure 3 illustrates a case of a glaucomatous eye that progressed by optic disc stereophotographs and VFs. The eye shows an apparent increase in GDx VCC RNFL thickness measurements over time, in disagreement with optic disc and VF findings. This could be explained by the worsening of atypical retardation patterns over time, as indicated by decreasing TSS scores. The TSS score changed from 70 on the baseline visit to 60 and 57 on subsequent visits. As a result, TSNIT average parameter values increased over time, from 47.0 μm in the baseline visit to 51.2 μm in the last visit.

Figure 4 illustrates a case of an eye that remained stable on optic disc stereophotographs and VFs, but showed apparent progression on GDx VCC. In this case, the disagreement also could be explained by changes in ARPs over time. The eye showed an apparent improvement in ARPs over time with increase in TSS scores. As a result, RNFL thickness measurements decreased over time, giving the impression of progression detected by the GDx VCC.

DISCUSSION

IN THE CURRENT STUDY, WE SHOWED THAT ATYPICAL patterns of retardation significantly affect detection of progressive RNFL loss with the GDx VCC scanning laser polarimeter. Changes in ARPs over time induced changes in RNFL thickness measurements that masked detection of RNFL loss in eyes with progressive disease and suggested progressive RNFL damage in eyes that in fact were stable.

Atypical retardation patterns first were described subjectively as scans showing irregular patches of elevated retardation values that would not match the expected retardation based on the current knowledge of RNFL anatomic features. A proprietary index, the TSS, was developed subsequently to quantify these patterns in scans obtained with the GDx VCC. Bagga and associates demonstrated that the TSS had excellent ability to discriminate atypical from typical scans originally classified based on subjective assessment by glaucoma experts.[10] They suggested that a cut-off of 80 would result in good specificity and sensitivity for detection of

atypical patterns. That is, eyes with a TSS of more than 80 would have minimal or no atypical patterns. ARPs have been shown to cause artifactual increase in measurements of RNFL thickness obtained with the GDx VCC.[10,11,17] TSS values are correlated with RNFL thickness measurements in the parapapillary area, with lower values of TSS (indicating more atypical scans) associated with thicker RNFL measurements. The artifactual increase in RNFL thickness decreases the ability of this instrument to detect RNFL damage in glaucomatous eyes with atypical scans. Bowd and associates investigated the impact of ARPs on the accuracy of the GDx VCC to discriminate glaucomatous from healthy eyes.[11] For the parameter NFI, they found that areas under the receiver operating characteristic curve decreased from 0.903 for eyes with no ARPs (TSS = 100) to 0.741 for eyes with severe ARPs (TSS = 20). Our findings showed that RNFL thickness measurements tended to increase in eyes with more ARPs. For baseline images, each 1 unit of TSS difference was associated with a 0.14-μm increase in RNFL average thickness among eyes.

Although previous cross-sectional investigations had suggested an effect of ARPs on GDx VCC RNFL thickness measurements, no study had yet investigated longitudinal changes in these patterns over time. It was reasonable to speculate that if these patterns do not change significantly over time, then the GDx VCC is still be useful to monitor the RNFL longitudinally, even in eyes with atypical scans. However, our study showed that eyes with atypical patterns had substantial variations in the amount of these patterns over time, as measured by the TSS. In eyes with more atypical patterns (TSS lower than 80), a change of more than 10 units in the value of TSS at follow-up compared with the baseline visit was seen in approximately half of the cases. This model also indicated that a 1-unit change in TSS score over time resulted in a 0.19-μm change in the average RNFL thickness. Therefore, a change of 10 units in TSS would result in a 1.9-μm change in RNFL thickness. The magnitude of these changes is high when compared with changes expected because of age-related decline of the RNFL or because of progressive glaucomatous damage. Therefore, variations in TSS measurements over time potentially can confound the assessment of progressive RNFL damage, as illustrated in Figures 3 and 4. It should be noted that although eyes with more atypical patterns of retardation tended to show more variation in TSS scores over time, these variations were not uniformly present in all of these eyes. Therefore, eyes with low TSS scores that maintained minimal or no TSS variations over time still would be candidates for RNFL monitoring using the GDx VCC.

The influence of TSS on detection of progressive RNFL loss was similar for the several GDx VCC parameters investigated in this study, with the exception of the TSNIT SD. For superior average and inferior average, a 1-unit change in TSS score over time induced changes of 0.13 and 0.11 μm, respectively. For the NFI parameter, a 1-unit change in TSS score induced a change of 0.20 units. The relationship between TSS changes and values of the TSNIT SD parameter over time, however, was not statistically significant. The TSNIT SD measures the variability of RNFL thickness in the circle of measurements around the optic disc. Because normal eyes have thicker RNFL in the superior and inferior sectors compared with the nasal and temporal ones, it is expected that they will show larger values of this parameter compared with normal eyes. However, the TSNIT SD has been shown to have low diagnostic accuracy compared with the other GDx VCC parameters for discriminating glaucomatous from healthy eyes. In this study, although this parameter was not significantly affected by TSS variations over time, it also was not able to discriminate progressing from nonprogressing eyes and, therefore, has little usefulness for longitudinal assessment of the RNFL.

In a previous study, we showed that the GDx VCC was able to identify progressive RNFL loss in eyes that had scans with minimal or no atypical patterns.[12] By excluding scans with TSS lower than 80, we showed that eyes that had progression on VFs, stereophotographs, or both had a higher average rate of decline in GDx VCC RNFL thickness than eyes that remained stable using these methods (0.70 μm/year vs 0.14 μm/year, respectively).[12] The average TSS

for all eyes in that sample was 95. These results are corroborated by the present investigation. For a lower average TSS score of 90, the rate of RNFL loss in eyes that progressed by VF, stereophotographs, or both was 0.65 μm/year compared with 0.19 μm/year for nonprogressing eyes, considering stable TSS score over time. These findings suggest that this instrument is useful to monitor RNFL loss in eyes that show minimal or no ARPs.

The reason for the variations in the severity of atypical patterns over time as found in this study is unclear. Although the origin of atypical patterns on GDx VCC scans is still a matter of debate, they seem to result from low signal-to-noise ratio caused by increased penetration of the laser beam into the strong birefringent sclera, which results in uncompensated retardation from the sclera being added to the RNFL retardation. Atypical patterns have been described more commonly in older subjects and in myopic eyes or eyes with light pigmented fundus.[18] The relationship between ARPs and age then could explain part of the results of our study. It is possible that aging would affect the penetration of laser light into the retina and result in worsening of atypical patterns from scleral interference. However, many eyes showed fluctuations in scores that are not consistent with a gradual aging effect. Also, many eyes showed improvement in the amount of atypical patterns from visit to visit. Although a change in our GDx instrument occurred during the study period, an analysis of the subgroup of eyes tested using only a single instrument revealed similar changes in TSS scores over time with similar impact on RNFL thickness measurements. It remains to be determined whether changes in testing conditions, corneal compensation, or instrument calibration and performance have any impact on changes in ARPs over time.

Recently, a new software-based algorithm called enhanced corneal compensation (ECC) has been developed to improve the signal-to-noise ratio while still achieving customized corneal compensation.[19] This method can be incorporated into the GDx VCC instrument and does not require changes to the hardware. The ECC was developed to improve neutralization of ARPs and to increase the dynamic range of the measurements in the low signal range. Studies comparing ECC and VCC methods for scanning laser polarimetry have shown improved diagnostic accuracy and better structure–function relationship in glaucoma with the new algorithm.[20–25] However, no longitudinal study has evaluated the GDx ECC for detection of progressive RNFL loss in glaucoma.

In conclusion, ARPs had a significant effect on detection of progressive RNFL loss with the GDx VCC. Eyes with large amounts of atypical patterns, great fluctuations, or both on these patterns over time may show changes in GDx VCC measurements that can appear falsely as glaucomatous progression or can mask true changes in the RNFL. Therefore, caution should be exercised when using the GDx VCC for longitudinal evaluation of the RNFL in eyes with ARPs.

Acknowledgments

THIS STUDY WAS SUPPORTED IN PART BY GRANTS N0. EY11008 (DR ZANGWILL) AND EY08208 (DR SAMPLE) FROM THE National Eye Institute, National Institutes of Health, Bethesda, Maryland. Dr Medeiros received honoraria and research support from Carl Zeiss Meditec Inc, and honoraria from Heidelberg Engineering. Dr Zangwill received honoraria and research support from Heidelberg Engineering and research support from Carl Zeiss Meditec Inc. Dr Sample received research support from Carl Zeiss Meditec Inc. Dr Weinreb is a consultant for Carl Zeiss Meditec Inc and Heidelberg Engineering. Involved in design and conduct of study (F.A.M., R.S.J., R.N.W.); collection, management, analysis, and interpretation of data (F.A.M., L.M.A.); and preparation, review, or approval of the manuscript (F.A.M., L.M.A., L.M.Z., P.A.S., R.S.J., R.N.W.). The University of California San Diego Human Subjects Committee approved all protocols and the methods described adhered to the tenets of the Declaration of Helsinki.

Biography

Biosketch

Felipe A. Medeiros, MD, is an Associate Professor of Ophthalmology at the Hamilton Glaucoma Center, University of California San Diego. His research interests include imaging of the optic disc and retinal nerve fiber layer, development of new methods for early detection of glaucoma, and elucidation of potential risk factors for development and progression of glaucoma.

REFERENCES

1. Weinreb RN, Dreher AW, Coleman A, et al. Histopathologic validation of Fourier-ellipsometry measurements of retinal nerve fiber layer thickness. Arch Ophthalmol 1990;108:557–560. [PubMed: 2322159]
2. Zhou Q, Weinreb RN. Individualized compensation of anterior segment birefringence during scanning laser polarimetry. Invest Ophthalmol Vis Sci 2002;43:2221–2228. [PubMed: 12091420]
3. Weinreb RN, Bowd C, Zangwill LM. Glaucoma detection using scanning laser polarimetry with variable corneal polarization compensation. Arch Ophthalmol 2003;121:218–224. [PubMed: 12583788]
4. Greenfield DS, Knighton RW, Feuer WJ, Schiffman JC. Normative retardation data corrected for the corneal polarization axis with scanning laser polarimetry. Ophthalmic Surg Lasers Imaging 2003;34:165–171. [PubMed: 12665235]
5. Medeiros FA, Zangwill LM, Bowd C, et al. Fourier analysis of scanning laser polarimetry measurements with variable corneal compensation in glaucoma. Invest Ophthalmol Vis Sci 2003;44:2606–2612. [PubMed: 12766063]
6. Medeiros FA, Zangwill LM, Bowd C, Weinreb RN. Comparison of the GDx VCC scanning laser polarimeter, HRT II confocal scanning laser ophthalmoscope, and Stratus OCT optical coherence tomograph for the detection of glaucoma. Arch Ophthalmol 2004;122:827–837. [PubMed: 15197057]

7. Medeiros FA, Zangwill LM, Bowd C, et al. Comparison of scanning laser polarimetry using variable corneal compensation and retinal nerve fiber layer photography for detection of glaucoma. Arch Ophthalmol 2004;122:698–704. [PubMed: 15136317]
8. Reus NJ, Lemij HG. Diagnostic accuracy of the GDx VCC for glaucoma. Ophthalmology 2004;111:1860–1865. [PubMed: 15465547]
9. Susanna, R., Jr; Medeiros, FA. Enhanced corneal compensation (ECC). In: Susanna, R., Jr; Medeiros, FA., editors. The Optic Nerve in Glaucoma. Cultura Medica; Rio de Janeiro, Brazil: 2006.
10. Bagga H, Greenfield DS, Feuer WJ. Quantitative assessment of atypical birefringence images using scanning laser polarimetry with variable corneal compensation. Am J Ophthalmol 2005;139:437–446. [PubMed: 15767051]
11. Bowd C, Medeiros FA, Weinreb RN, Zangwill LM. The effect of atypical birefringence patterns on glaucoma detection using scanning laser polarimetry with variable corneal compensation. Invest Ophthalmol Vis Sci 2007;48:223–227. [PubMed: 17197536]
12. Medeiros FA, Alencar LM, Zangwill LM, et al. Detection of progressive retinal nerve fiber layer loss in glaucoma using scanning laser polarimetry with variable corneal compensation. Invest Ophthalmol Vis Sci 2009;50:1675–1681. [PubMed: 19029038]
13. Weinreb RN, Shakiba S, Zangwill L. Scanning laser polarimetry to measure the nerve fiber layer of normal and glaucomatous eyes. Am J Ophthalmol 1995;119:627–636. [PubMed: 7733188]
14. Leske MC, Heijl A, Hussein M, et al. Factors for glaucoma progression and the effect of treatment: the Early Manifest Glaucoma Trial. Arch Ophthalmol 2003;121:48–56. [PubMed: 12523884]
15. Cnaan A, Laird NM, Slasor P. Using the general linear mixed model to analyse unbalanced repeated measures and longitudinal data. Stat Med 1997;16:2349–2380. [PubMed: 9351170]
16. Feldman HA. Families of lines: random effects in linear regression analysis. J Appl Physiol 1988;64:1721–1732. [PubMed: 3379003]
17. Da Pozzo S, Marchesan R, Canziani T, et al. Atypical pattern of retardation on GDx VCC and its effect on retinal nerve fibre layer evaluation in glaucomatous eyes. Eye 2006;20:769–775. [PubMed: 16021190]
18. Lemij HG, Reus NJ. New developments in scanning laser polarimetry for glaucoma. Curr Opin Ophthalmol 2008;19:136–140. [PubMed: 18301287]
19. Reus NJ, Zhou Q, Lemij HG. Enhanced imaging algorithm for scanning laser polarimetry with variable corneal compensation. Invest Ophthalmol Vis Sci 2006;47:3870–3877. [PubMed: 16936099]
20. Bowd C, Tavares IM, Medeiros FA, et al. Retinal nerve fiber layer thickness and visual sensitivity using scanning laser polarimetry with variable and enhanced corneal compensation. Ophthalmology 2007;114:1259–1265. [PubMed: 17289147]
21. Choi J, Kim KH, Lee CH, et al. Relationship between retinal nerve fibre layer measurements and retinal sensitivity by scanning laser polarimetry with variable and enhanced corneal compensation. Br J Ophthalmol 2008;92:906–911. [PubMed: 18577640]
22. Kim KH, Choi J, Lee CH, et al. Relationship between scanning laser polarimetry with enhanced corneal compensation and with variable corneal compensation. Korean J Ophthalmol 2008;22:18–25. [PubMed: 18323701]
23. Mai TA, Reus NJ, Lemij HG. Diagnostic accuracy of scanning laser polarimetry with enhanced versus variable corneal compensation. Ophthalmology 2007;114:1988–1993. [PubMed: 17459481]
24. Mai TA, Reus NJ, Lemij HG. Structure-function relationship is stronger with enhanced corneal compensation than with variable corneal compensation in scanning laser polarimetry. Invest Ophthalmol Vis Sci 2007;48:1651–1658. [PubMed: 17389496]
25. Medeiros FA, Bowd C, Zangwill LM, et al. Detection of glaucoma using scanning laser polarimetry with enhanced corneal compensation. Invest Ophthalmol Vis Sci 2007;48:3146–3153. [PubMed: 17591884]

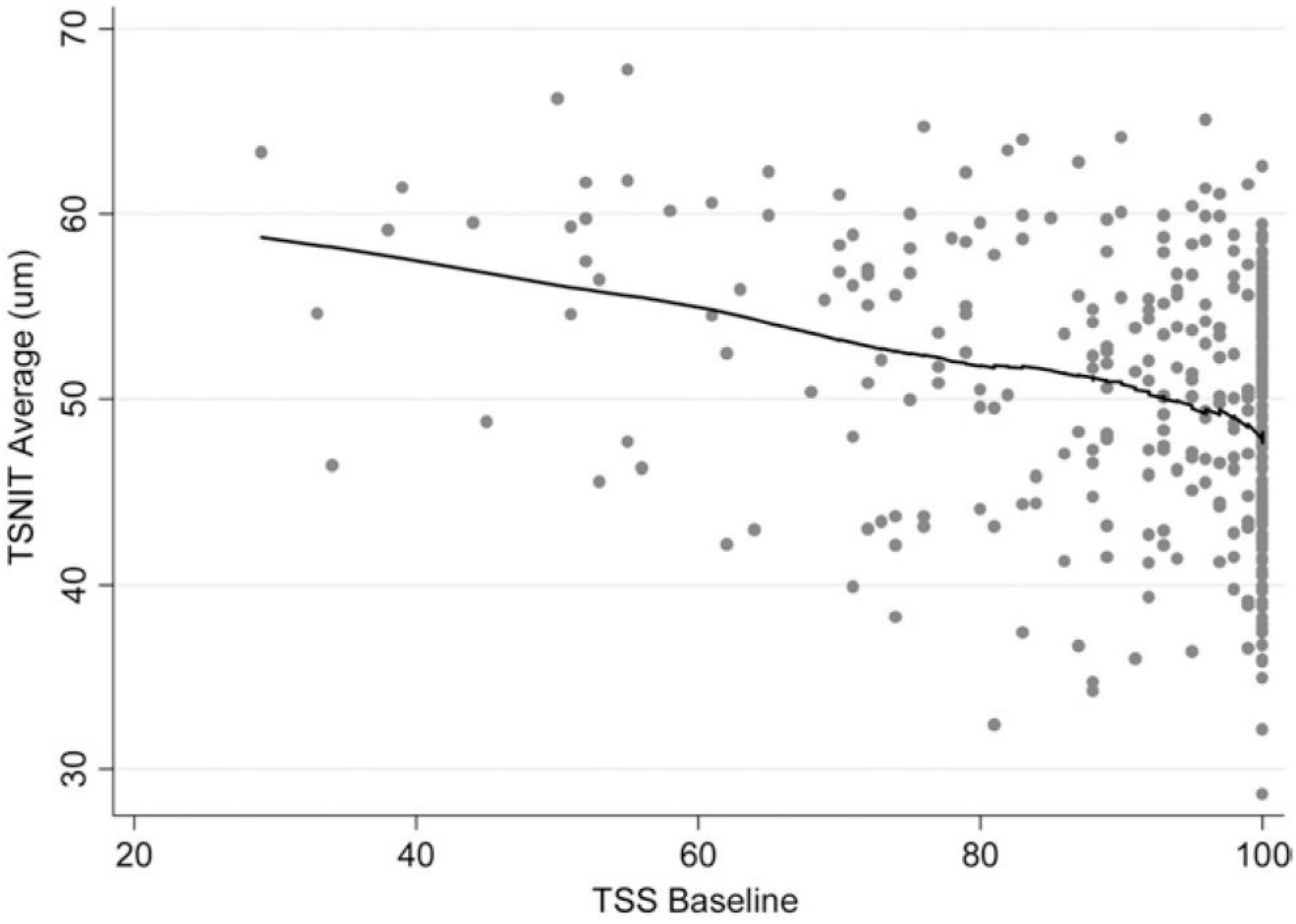

FIGURE 1.
Scatterplot showing the relationship between typical scan scores (TSS) at baseline and temporal–superior–nasal–inferior–temporal (TSNIT) average values at baseline. Lower TSS values were associated with higher TSNIT average measurements. A locally weighted scatterplot smoother (LOWESS) shows that the relationship between TSS and TSNIT average values was approximately linear.

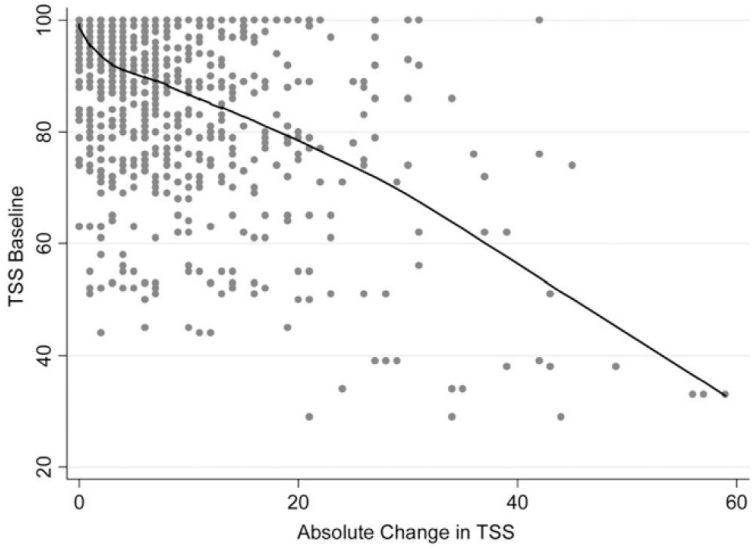

FIGURE 2.

Scatterplot showing the relationship between absolute change in TSS over time and baseline TSS scores. Lower TSS scores at baseline had greater absolute changes in TSS scores over time. A LOWESS shows that the relationship was approximately linear.

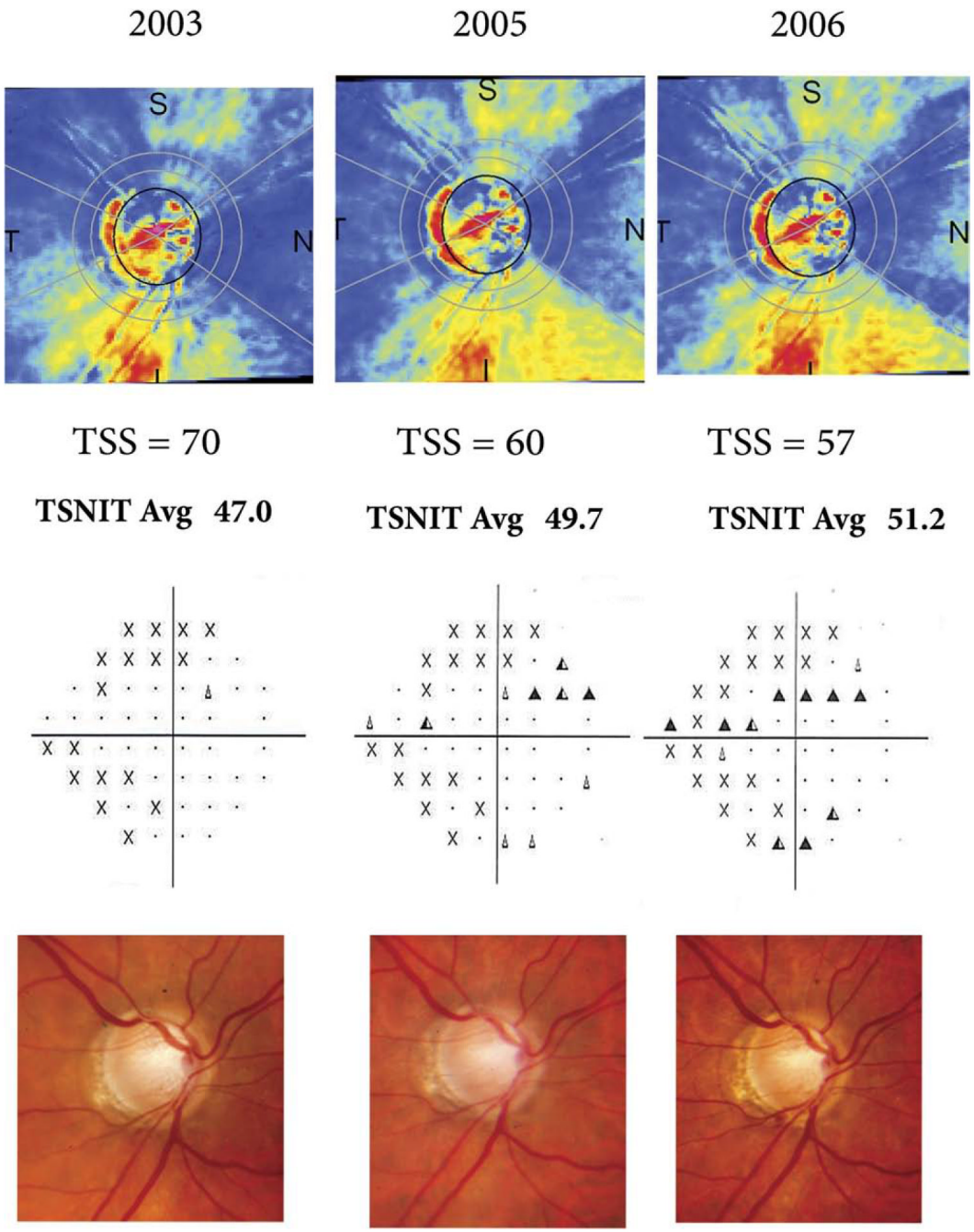

FIGURE 3.

GDx variable corneal compensation (VCC) scans (Top) of a glaucomatous eye that progressed by visual fields (VF; Middle) and optic disc stereophotographs (Bottom). The optic disc photographs show progressive inferior neuroretinal rim thinning with associated disc hemorrhages. The VFs show corresponding worsening on the superior hemifield. However, GDx VCC scans show an apparent increase in retinal nerve fiber layer (RNFL) thickness measurements over time as indicated by the parameter TSNIT average, in disagreement with optic disc and VF findings. This could be explained by the worsening of atypical retardation patterns over time, as indicated by decreasing TSSs.

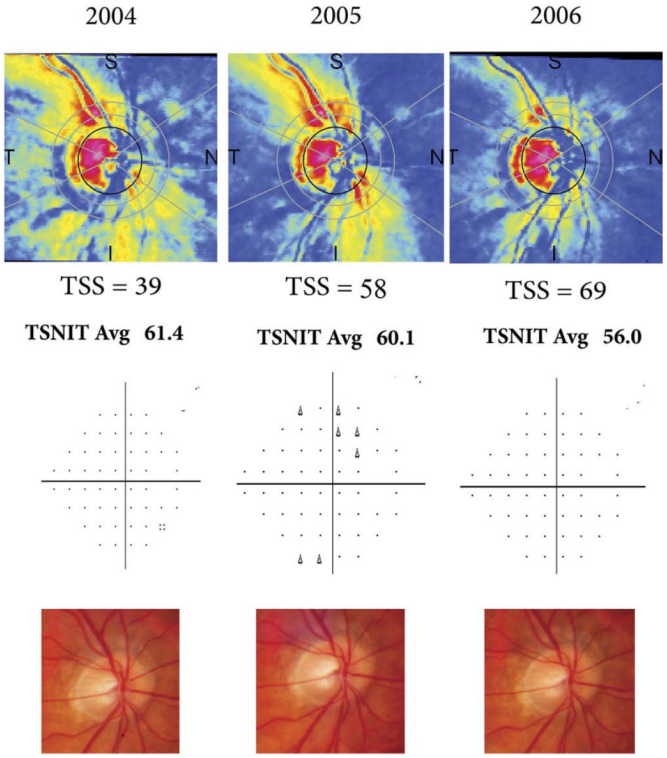

FIGURE 4.

GDx VCC scans (Top) of an eye that remained stable on VFs (Middle) and optic disc stereophotographs (Bottom). The GDx VCC scans show an improvement in the amount of atypical patterns with an apparent decrease in RNFL thickness measurements over time.

TABLE 1

Results of the Random-Coefficients Model to Investigate the Influence of Atypical Retardation Patterns on Changes of the GDx VCC Parameter Temporal–Superior–Nasal–Inferior–Temporal Average over Time

Parameter	Coefficient	Estimate	95% CI	*P* value
Intercept	β_0	50.1	(49.8 to 50.3)	< .001
TSS[a]	β_1	−0.006	(−0.027 to 0.014)	.544
TSS × TIME	β_2	−0.009	(−0.015 to −0.002)	.015
ΔTSS	β_3	−0.19	(−0.20 to −0.18)	< .001
PROG	β_4	0.32	(−0.56 to 1.19)	.480
TIME	β_5	−0.19	(−0.29 to −0.08)	< .001
PROG × TIME	β_6	−0.46	(−0.75 to −0.18)	.002
BASELINE	β_7	0.99	(0.94 to 1.03)	< .001
BASELINE × TIME	β_8	−0.03	(−0.05 to −0.02)	< .001

CI = confidence interval; PROG = variable indicating progression by standard methods (1 = yes, 0 = no); TSNIT = temporal–superior–nasal–inferior–temporal; TSS = typical scan scores; VCC = variable corneal compensation.

[a]The variable TSS (typical scan score) was centered on its mean value (90). See text for description of the variables in the model.

TABLE 2

Results of the Random-Coefficients Models to Investigate the Influence of Atypical Retardation Patterns on Changes of the GDx VCC Parameters Superior Average, Inferior Average, Nerve Fiber Indicator, and Temporal–Superior–Nasal–Inferior–Temporal Standard Deviation

	Superior Average		Inferior Average		NFI		TSNIT SD	
Parameter	**Estimate**	***P* value**	**Estimate**	***P* value**	**Estimate**	***P* value**	**Estimate**	***P* value**
Intercept	59.3	< .001	58.2	< .001	28.7	< .001	20.5	< .001
TSS[a]	−0.017	.264	−0.002	.897	0.006	.798	0.008	.473
TSS × TIME	−0.008	.129	−0.015	.005	0.015	.094	−0.0002	.946
ΔTSS	−0.13	< .001	−0.11	< .001	0.20	< .001	−0.003	.567
PROG	0.36	.611	0.03	.966	−0.44	.699	−0.45	.367
TIME	−0.24	.003	−0.14	.096	0.40	.006	−0.14	.008
PROG × TIME	−0.58	.009	−0.63	.014	1.46	< .001	−0.23	.135
BASELINE	0.98	< .001	0.95	< .001	0.98	< .001	0.92	< .001
BASELINE × TIME	−0.03	< .001	−0.03	< .001	−0.03	< .001	−0.04	< .001

CI = confidence interval; NFI = nerve fiber indicator; PROG = variable indicating progression by standard methods (1 = yes, 0 = no); SD = standard deviation; TSNIT = temporal–superior–nasal–inferior–temporal; TSS = typical scan scores; VCC = variable corneal compensation.

[a]The variable TSS was centered on its mean value (90). See text for description of the variables in the model.